ELSEVIER

Available online at www.sciencedirect.com

SCIENCE DIRECT®

Journal of Nuclear Materials 340 (2005) 299–306

journal of nuclear materials

www.elsevier.com/locate/jnucmat

Self-reduction of dioxoplutonium VI: Characterization and modeling of radiolytic and disproportionation pathways

John M. Haschke *

Actinide Science Consulting, 11003 Willow Bend Drive, Waco, TX 76712, USA

Received 24 August 2004; accepted 7 December 2004

Abstract

Kinetic modeling shows that self-reduction of dioxoplutonium VI is consistent with disproportionation of Pu(VI) and reaction of the Pu(VII) product with water, as well as with alpha-particle radiolysis of water and reaction of products with Pu(VI). Comparison of predicted and observed [Pu(VI)]–time data confirms that self-reduction of ^{238}Pu(VI) at pH 0 is induced by radiolysis, but that self-reduction reactions of ^{239}Pu(VI) at pH 1.5 and ^{242}Pu(VI) at pH 6 are driven by disproportionation. Modeling of [Pu(VI)]–time behavior of solutions containing ^{210}Po as an alpha source shows that control of the reduction path changes from disproportionation to radiolytic over time at pH 0.7. Self-reduction of Pu(VI) consistently follows the most rapid path as determined by pH, Pu(VI) concentration, and the isotopic state of Pu. Chemistry and kinetics of the processes by which Pu(VI) self-reduction drives the decrease in average oxidation number of plutonium-containing solutions over time are discussed.

1. Introduction

Spontaneous reduction of Pu(VI) to Pu(V) in aqueous solution is well known and occurs over a wide pH range. Chemistry and kinetics of the process are addressed by recent letters in this journal [1,2]. Newton and Hobart [1] conclude that reduction of $^{239}PuO_2^{2+}$ in solutions with pH values less than 2.2 results from reaction with H_2O_2 and other reducing agents formed by alpha-induced radiolysis of water, but are unable to account for self-reduction of Pu(VI) at pH 6. Peroxide reduction of Pu(VI) is described as follows:

$$2PuO_2^{2+}(aq) + H_2O_2(aq) \rightarrow 2PuO_2^{+}(aq) + 2H^{+}(aq) + O_2(g) \quad (1)$$

Combination of Eq. (1) with that for formation of H_2O_2 by radiolysis of H_2O yields the net reduction reaction:

$$PuO_2^{2+}(aq) + \tfrac{1}{2}H_2O(l) \rightarrow PuO_2^{+}(aq) + H^{+}(aq) + \tfrac{1}{4}O_2(g) \quad (2)$$

A first-order dependence of the Pu(VI) reduction rate on [Pu(VI)] derived by evaluation of experimental [Pu(VI)]–time data is cited as evidence that self-reduction of ^{239}Pu at pH 1.5 is radiolysis-induced [1].

Radiolysis-induced reduction for ^{239}Pu(VI) is challenged in an accompanying letter that describes use of quantitative kinetic modeling to identify the reduction pathway [2]. The [^{239}Pu(VI)]–time curve calculated for

---

* Tel.: +1 254 399 0740; fax: +1 254 399 8876.
E-mail address: johnhaschke@msn.com

0022-3115/$ - see front matter © 2005 Elsevier B.V. All rights reserved.
doi:10.1016/j.jnucmat.2004.12.011

simultaneous radiolytic formation of H_2O_2 and reaction of product peroxide with Pu(VI) at pH 1.5 does not agree with observation and shows that the rate of radiolysis-induced reduction is independent of [Pu(VI)]. The experimental dependence of $-d[Pu(VI)]/dt$ on [Pu(VI)] is either first order [1] or second-order [3]. The [Pu(VI)]–time curve calculated using a second-order rate law agrees with experimental data. This result and similarities in kinetic behavior of PuO_2^{2+} and PuO_2^{+} [2] support the conclusion that Pu(VI) instability, like that of Pu(V), is driven by disproportionation:

$$2PuO_2^{2+}(aq) \rightarrow PuO_2^{+}(aq) + PuO_2^{3+}(aq) \qquad (3)$$

Disproportionation is isotope insensitive and controlled by kinetics, but the chemistry is uncertain. Although Pu(VII) is stable and characterized in basic solution, its speciation in neutral and acidic media is undefined. Formulation of the reaction is precluded by this lack of knowledge. The PuO_2^{2+} (aq) and PuO_2^{3+} (aq) formulas in Eq. (3) are adopted for convenience. However, the undefined, but transient, Pu(VII) product is highly unstable and reacts immediately with water to reform Pu(VI) [4]. The net reaction is also described by Eq. (2).

Peroxide reduction of Pu(VI) is well documented [5,6] and H_2O_2 is the primary product of alpha radiolysis [7], but [Pu(VI)]–time data for ^{239}Pu(VI) [8] and ^{242}Pu(VI) [9] show that self-reduction is most rapid near zero time. At that point, concentrations of H_2O_2 and other radiolytic reductants are low and reduction of Pu(VI) should be slow. Modeling of ^{239}Pu(VI) reduction by radiolytic H_2O_2 confirms this discrepancy [2], but is limited to evaluation of a single experimental condition. Objectives of this study are to evaluate the adequacy of modeling assumptions, to extend modeling calculations to Pu(VI) solutions with other isotopes and pH values, and to define conditions that determine the course of Pu(VI) self-reduction. Conclusions are tested by reevaluating results of a classic study in which ^{210}Po was used as alpha source to promote Pu(VI) reduction [10].

2. Data and methods

Experimental data used in this study are derived from graphical sources in the literature. The data set includes [Pu(VI)]–time results for ^{238}Pu(VI) in perchlorate solution at pH 0 [11], for ^{239}Pu(VI) in perchlorate solution at pH 1.5 [8], and for ^{242}Pu(VI) in high-purity water at pH 6 [9]. Similar results for a solution containing an unspecified Pu(VI) isotope and ^{210}Po at pH 0.7 [10] are also evaluated. Estimated errors in concentration and time are ±5% of the derived values and have insignificant effect on comparisons of observations with modeling predictions.

Peroxide formation accounts for 80% of alpha-induced reductive capacity [7] and radiolysis-induced reduction of Pu(VI) is approximated by modeling kinetic behavior of Eq. (1). The radiolytic H_2O_2 formation rate, $+R_{H_2O_2}$, is a constant calculated for each solution using known half lives and α-particle energies of Pu isotopes, initial Pu(VI) concentrations, $[Pu(VI)]_0$, and the G value (0.985) for radiolysis of water [7]. The rate law for H_2O_2 reduction of Pu(VI) is $-d[Pu(VI)]/dt = k[Pu(VI)][H_2O_2]/[H^+]$ with an average k of 0.5 min^{-1} at room temperature [5]. Radiolytic Pu(VI) reduction rates, $-R_r$, and peroxide reaction rates, $-R_{H_2O_2}$, as well as dynamic concentrations of Pu(VI) and H_2O_2, are calculated as a function of time by iterative numerical integration of the combined rate expression for peroxide formation and Pu(VI) reduction. Unless otherwise stated, calculations are based an initial peroxide concentration, $[H_2O_2]_0$, of zero and on reduction of two Pu(VI) ions per H_2O_2. As discussed in Section 3.1.1, the later assumption results in over-estimation of the radiolytic.

Concern exists about using the H_2O_2–Pu(VI) rate law beyond the pH range of derivation (pH −1 to 1) [5]. Predicted rates of H_2O_2 consumption for ^{239}Pu and ^{242}Pu at high pH are consistently larger than the calculated rates of radiolytic peroxide formation. Therefore, predicted rates of Pu(VI) self-reduction are determined by pH-independent maximum rates of radiolytic H_2O_2 formation. Rate-law applicability is of concern only if the rate of peroxide formation exceeds the rate of consumption via Eq. (1).

Disproportionation-induced self-reduction of Pu(VI) via Eq. (3) is modeled using the second-order rate law $-d[Pu(VI)]/dt = k_{VI}[Pu(VI)]^2$ proposed in earlier studies [2,3]. The isotopic state of Pu is not a factor. Values of k_{VI} used in the initial calculations at each pH are assumed equal to k_V for disproportionation of Pu(V) to Pu(IV) and Pu(VI) at that $[H^+]$ (Section 3.2.1). As in the case of radiolytic reduction, the disproportionation-induced reduction rate, $-R_d$, and the dynamic [Pu(VI)] are derived as functions of time by iterative numerical integration of the rate law. Final k_{VI} values obtained by systematic variation of the constant to minimize the difference between observed and predicted [Pu(VI)]–time data are consistently less than k_V by a factor of 4.

Identification of the apparent reaction path is based on comparison of observed and predicted [Pu(VI)]–t data and on n, the order of reaction with respect to [Pu(VI)]. Values of n are integers defined by the slopes of $\ln R$–$\ln[Pu(VI)]$ [2,3]. This method of deriving n is applicable if Pu(VI) is the only reactant or if concentrations of other reactants are invariant. In some cases, n values obtained from calculated reduction rates and Pu(VI) concentrations are used to test for calculational error.

3. Results and discussion

3.1. Alpha-induced self-reduction of Pu(VI)

3.1.1. Formation and reaction of radiolytic products

Important products formed by alpha radiolysis of water and their anticipated interactions with Pu(VI) are described by Pagès [10]. Quantitative assessment of the consequences of radiolysis is contingent on availability of measured molecular yields for relevant reactions. Recently compiled G values for radiolytic products [7] and their anticipated redox reactions with Pu(VI) are given in Table 1.

As outlined previously [10], the $G_{\mathrm{Pu(VI)}}$ for reduction of Pu(VI) to Pu(V) is defined by the sum of G values for H_2O_2, OH, HO_2, and H. Values for H_2 and H^+, as well as for O_2 formed by reaction of H_2O_2 and HO_2, are excluded because those species are unreactive with Pu(VI). A maximum theoretical $G_{\mathrm{Pu(VI)}}$ of 2.22 equivalents per 100 eV of adsorbed energy is obtained if only reducing species in Table 1 are considered. This value is closely approximated in modeling calculations by assuming that each peroxide reduces two Pu(VI) ions Eq. (1). Electrons are readily lost to reactions other than Pu(VI) reduction and the likelihood of each H_2O_2 reducing more than one Pu(VI) is remote. Therefore, the most likely $G_{\mathrm{Pu(VI)}}$ is 1.18 equivalents per 100 eV of absorbed energy.

Table 1
G values for products of alpha-particle radiolysis of water [7] and anticipated redox half reactions of those products with Pu(VI)

Radiolysis product	G value (molecules per 100 eV)	Redox reaction
H_2	1.3	Unreactive
H_2O_2	0.985	$H_2O_2 \rightarrow 2e^- + 2H^+ + O_2$
OH	0.24	$OH + e^- \rightarrow OH^-$
HO_2	0.22	$HO_2 \rightarrow e^- + H^+ + O_2$
H	0.21	$H \rightarrow e^- + H^+$
e^-	0.06	$e^- \rightarrow e^-$
H^+	0.06	Unreactive

3.1.2. Modeling and evaluation of radiolysis-induced Pu(VI) self-reduction

Experimental [Pu(VI)]–t data for self-reduction of 9.7 mM ^{239}Pu(VI) at pH 1.5 [8] show that [Pu(VI)] decreases at a rate that progressively slows until a steady-state concentration near 1 mM is reached after 250 days. Kinetic evaluation for the first 40 days is unambiguous because 63% of the Pu(VI) is reduced to Pu(V) during that period without reaction of the Pu(V) product. Onset of Pu(V) disproportionation and reformation of Pu(VI) at a rate faster than the loss rate at day 40 has no detectable effect on the [Pu(VI)]–time curve. Modeling of radiolysis-induced reduction [2] predicts that H_2O_2 accumulates in solution and $-R_r$ increases during an initial 35 min period. Thereafter, the rate of peroxide consumption is limited by its rate of formation and [Pu(VI)] decreases at a radiolysis-controlled constant rate ($8.0 \times 10^{-5}\ \mathrm{mol\,l^{-1}\,d^{-1}}$) that is independent of [Pu(VI)] ($n = 0$). The predicted time to reach 63% reduction is 76 days. Elimination of Pu(VI) by the thermodynamically favorable Pu(VI)–H_2O_2 reaction is expected after 121 days. If $G_{\mathrm{Pu(VI)}}$ is 1.18, $-R_r$ is constant at $4.6 \times 10^{-5}\ \mathrm{mol\,l^{-1}\,d^{-1}}$ and complete reaction is expected after 210 days. Lack of agreement between predicted and observed behavior implies that self-reduction is not radiolysis-induced, but predictions may be altered by assumptions.

Peroxide concentrations present during reduction were not reported [8] and the value adopted for $[H_2O_2]_0$ may significantly influence model predictions. Effects of initial peroxide concentration on the kinetics of reducing a 9.7 mM ^{239}Pu(VI) solution at pH 1.5 via Eq. (1) are compared in Table 2. $[H_2O_2]_0$ is an important determinant of kinetic behavior, but varying that parameter does not bring agreement between observation and prediction at any point. The initial reduction rate is matched by increasing $[H_2O_2]_0$ to 1 μM, but behavior is ultimately identical to that for $[H_2O_2]_0 = 0$ after a brief adjustment period. A false second-order dependence on Pu(VI) is observed for $[H_2O_2]_0 = 5$ mM because simultaneous changes in concentrations of both reactants work in concert. A first-order dependence is observed only if $[H_2O_2]_0$ is so large that the $[H_2O_2]$ remains essentially constant during reaction. That condition is unlikely to exist near zero time.

Other observations are also inconsistent with expectation. Alpha-induced reaction is identified as the source of ^{239}Pu(VI) self-reduction, but the steady state existing from day 250 until termination of measurements near day 400 is attributed to chemical equilibrium established by disproportionation of Pu(V) : $2PuO_2^+(aq) = PuO_2^{2+}(aq) + PuO_2$ (colloid) [8]. Equilibrium control changes only if this reaction becomes thermodynamically more favorable than Eq. (1). Accumulation of radiolytic peroxide increases the $[H_2O_2]$ to approximately 0.01 M at day 400. Combination of this result with reference data, [12,13], and measured steady-state plutonium concentrations at pH 1.5 [8] gives a ΔG of $-66\ \mathrm{kJ\,mol^{-1}}$ for Eq. (1) at that point. The proposed equilibrium reaction at pH 1.5 is accurately described by Eq. (4) [11]:

$$2PuO_2^+(aq) + 2H^+(aq) = Pu(OH)_2^{2+}(aq) + PuO_2^{2+}(aq). \quad (4)$$

Evaluation based on the Pu(IV) concentration in equilibrium with hydrous oxide at pH 1.5 [6], measured

Table 2
Comparison of observed kinetic parameters with values calculated for radiolysis-induced Eq. (1) and disproportionation-induced (Eq. (3)) self-reduction of a 9.7 mM ^{239}Pu(VI) solution at pH 1.5

Kinetic result	Observed	Predicted for Eq. (1) $[H_2O_2]_0$ (M)				Predicted for Eq. (3)
		0	1×10^{-6}	5×10^{-3}	0.10	
Time to $[H_2O_2]_0$ [a]	–	0	35 min	123 d	6.8 y	–
Initial $-R$ (mol Pu(VI) l^{-1} d^{-1}) [b]	2×10^{-4}	3×10^{-6}	2×10^{-4}	1.1	22	3×10^{-4}
Adjustment period (min) [c]	0	35	60	0	0	0
$-R$ after adjustment (mol Pu(VI) l^{-1} d^{-1}) [b]	2×10^{-4}	8×10^{-5}	8×10^{-5}	1.1	22	3×10^{-4}
Time to 63% reaction [d]	41 d	76 d	76 d	18 min	40 s	40 d
n	1 or 2 [e]	0	0	2.0	1.0	2.0

[a] The time period required to form the indicated $[H_2O_2]_0$ is calculated for a 9.7 mM ^{239}Pu solution in which peroxide is not lost to reaction or decomposition.

[b] $-R$ is a generic symbol for the rate of Pu(VI) self-reduction by radiolysis or disproportionation. The initial rate is calculated for an elapsed time of one minute.

[c] The adjustment time is the period required for onset of sustained Pu(VI) reduction or for the $[H_2O_2]$ to become stable.

[d] Time in years, days, minutes, and seconds are indicated by y, d, min and s, respectively.

[e] The exponent n of the [Pu(VI)] is an integer. A value of $n = 1.26$ is derived by Newton and Hobart [1]; a value of $n = 2$ is obtained by Haschke and Oversby [3].

steady-state Pu(V) and Pu(VI) concentrations [8] corrected for ionic strength effects [12], and reference data [12] gives a ΔG of +13 kJ mol^{-1} for Eq. (4). If Pu(VI) is reduced by radiolytic H_2O_2, that reaction should continue beyond the observed steady state and result in an equilibrium [Pu(V)]/[Pu(VI)] ratio (>10^4) that far exceeds the experimental value (0.4). Control of the system by another process is apparent because neither Eq. (1) nor Eq. (4) accounts for the observed steady state [3]. Dependence of measured reaction quotients on the amount of plutonium-containing solid coexisting with a steady-state solution suggests that the system is controlled by kinetics [14].

Observed concentration–time data for self-reduction of 0.1 mM ^{242}Pu(VI) at pH 6 [9] are similar to those for ^{239}Pu(VI) at pH 1.5. The [Pu(VI)] decreases at a progressively slower rate over time. Reduction is approximately 10% complete after 7 days and about 60% complete after 110 days. The theoretical $+R_{H_2O_2}$ is 5.4×10^{-8} mol l^{-1} d^{-1}, but the effective rate is 1.0×10^{-7} mol l^{-1} d^{-1} because the alpha activity of the sample was doubled by ^{238}Pu contamination. Modeling shows that $[H_2O_2]$ and $-R_r$ increase during an initial five-second period. The maximum reduction rate is constant (2×10^{-7} mol l^{-1} d^{-1}) because $-R_{H_2O_2}$ is limited by $+R_{H_2O_2}$. A period of 45 days is predicted for reaching 10% reaction. If calculation is based on $G_{Pu(VI)} = 1.18$, 10% reduction is expected at 77 days. The predicted n for radiolysis-induced reduction is zero, but the observed value is 2 [1–3]. Radiolysis-induced reaction does not account for behavior.

Limited [Pu(VI)]–time data for self-reduction of 1.1 mM ^{238}Pu(VI) at pH 0 show a relatively rapid reaction that is 95% complete after 7 days [11]. The theoretical $+R_{H_2O_2}$ is 1.5×10^{-3} mol l^{-1} d^{-1}. Modeling shows that $[H_2O_2]$ and $-R_r$ increase initially as peroxide accumulates in solution and that the radiolytic H_2O_2 formation rate exceeds the rate at which peroxide is consumed via Eq. (1). The predicted $-R_r$ continues to increase until the reaction is 40% complete after about 1 day, but progressively slows beyond that point as the [Pu(VI)] decreases. The resulting [Pu(VI)]–time curve is sigmoidal.

Table 3
Comparison of measured [^{238}Pu(VI)]–time data [11] with values calculated for radiolysis-induced and disproportionation-induced reduction of Pu(VI)

Elapsed time (days)	[Pu(VI)] (mM)			
	Observed	Radiolysis [a]		Disproportionation
		100%	25%	
0	1.10	1.10	1.10	1.10
1	–	0.96	1.06	0.80
2	–	0.29	0.91	0.64
2.7	0.57	0.04	0.72	0.56
3	–	0.01	0.67	0.54
4	–	0.00	0.44	0.47
5	–	0.00	0.27	0.41
6	–	0.00	0.14	0.36
6.9	0.05	0.00	0.05	0.34
7	–	0.00	0.05	0.33
10	–	0.00	0.00	0.25
15	–	0.00	0.00	0.17
16.9	0.03	0.00	0.00	0.15
20	–	0.00	0.00	0.13

[a] Values for 100% are calculated with the theoretical $+R_{H_2O_2}$ based on pure ^{238}Pu and absorption of all alpha energy by water; values for 25% are calculated assuming that $+R_{H_2O_2}$ is a factor of four less than theoretical.

Comparison of calculated and measured data in Table 3 shows that the predicted reaction rate is more rapid than observed and that reaction reaches 95% completion after only 2.2 days.

Model parameters were systematically varied in an effort to identify a likely explanation for the slower-than-expected reduction rate of ^{238}Pu(VI). Attempts to appropriately slow the rate and match observed [Pu(VI)]–time data using reduced values of k were unsuccessful. However, general agreement (Table 3) is achieved with a $+R_{H_2O_2}$ rate that is 25% of theoretical, implying that only a fraction of the plutonium was ^{238}Pu or that only a fraction of the alpha energy was absorbed by water. Continuing reduction by H_2O_2 is expected to drive the [Pu(VI)] below detectable limits within 10 days, but observation of a measurable concentration after 17 days suggests that a steady state is established. Derivation of n by $\ln(-R_r)$–ln[Pu(VI)] analysis of modeling results gives apparent values of -6 during the initial 30% of reaction and 0.6 for 30% to 90% of reaction. Results are consistent with radiolysis-induced reduction, but the proposed first-order dependence of $-R_r$ on [Pu(VI)] [1] is not observed.

3.2. *Disproportionation-induced self-reduction of Pu(VI)*

3.2.1. *The concept of disproportionation-induced Pu(VI) self-reduction*

The kinetics of Pu(VI) self-reduction and Pu(V) disproportionation are remarkably similar. Measured [Pu(V)]–time and [Pu(IV)]–time curves for pH 1.5–1.6 [8] are in close agreement when compared over the same ranges of Pu(V) and Pu(VI) concentration. Kinetics of both reactions are described by second-order rate laws [2,3]. The second-order rate constants, k_V for Pu(V) and k_{VI} for Pu(VI), have nearly identical values [3] and pH dependencies [2]. The similarities of linear ln([dPu(V)]/dt)–ln[Pu(V)] and ln(d[Pu(VI)]/dt)–ln[Pu(VI)] data at pH 0–6 [3] support the conclusion that self-reduction of Pu(VI) is driven by disproportionation.

Disproportionation of Pu(VI) is not expected because the Gibbs energy of forming Pu(V) and Pu(VII) via Eq. (3) is unfavorable. However, ΔG for disproportionation of Pu(V) to form Pu(IV) and Pu(VI) (Eq. (4)) is also unfavorable. Calculations involving measured concentrations [8] and specific ion interaction theory to correct for ionic-strength effects [12] show that ΔG for disproportionation of 28 mM PuO_2^+ to $Pu(OH)_2^{2+}$ and PuO_2^{2+} at pH 1.6 varies from $-14\ \mathrm{kJ\,mol^{-1}}$ at 1% completion to $+13\ \mathrm{kJ\,mol^{-1}}$ at steady state (98% completion). Continuation of reaction after the Gibbs energy became positive is also observed for disproportionation of 0.3 mM PuO_2^+ to form $Pu(OH)_4^0$ and $PuO_2(OH)_2^0$ at pH 7.1 [15]. ΔG varies from $-13\ \mathrm{kJ\,mol^{-1}}$ to $+16\ \mathrm{kJ\,mol^{-1}}$. In both cases, Pu(V) disproportionates despite a positive Gibbs energy, implying that disproportionation of Pu(VI) is also possible if both reactions are controlled by kinetics instead of thermodynamics.

The proposed mechanisms for disproportionation of PuO_2^+ and PuO_2^{2+} account for occurrence of reactions with unfavorable Gibbs energies and for similar kinetic behavior [2]. Formation of hydrox-bridged dimers is suggested by observed pH dependencies of k_V and k_{VI}, as well as by proportionality of the Pu(V) disproportionation rate to $[Pu(V)]^2$ and proportionality of the Pu(VI) self-reduction rate to $[Pu(VI)]^2$. Quantum tunneling [16] creates a finite probability of instantaneously forming Pu(IV) and Pu(VI) in Pu(V) dimers and Pu(V) and Pu(VII) in Pu(VI) dimers. Observed disproportionation reactions of Pu(V) and Pu(VI) are consistent with kinetically controlled dissociation of labile dimers in asymmetric electron states. Reverse rates are negligible because Pu(IV) precipitates as hydrous oxide and Pu(VII) reacts immediately with water.

Feasibility of a kinetically controlled disproportionation mechanism is supported by isotopic tracer studies of electron exchange between Pu(III) and Pu(IV) at pH -0.3 to 0.4 [17]. Pu^{3+}(aq) and $PuOH^{3+}$ (aq) predominate in solution and the rate law for exchange (rate = $k^*[Pu^{3+}][PuOH^{3+}]$) shows an inverse dependence of k^* on $[H^+]$. At pH 0, the electron exchange rate is 10^2 faster than the disproportionation rates of Pu(V) and Pu(VI) [2] and is consistent with the proposed kinetic process. Involvement of a labile hydroxo dimer in the Pu(III)–Pu(IV) exchange and a redox mechanism based on transfer of an OH group are suggested [17].

Parallels between the pH dependencies of k_V and k_{VI} provide a method for estimating second-order rate constants of Pu(VI) disproportionation at pH 0–7. Values of k_{VI} in this pH range are consistently a factor of 4 less than those of k_V. Equations describing the dependence of k_V on $[H^+]$ [2] are given in Table 4, but their utility for predicting k_{VI} values in basic media is uncertain.

3.2.2. *Modeling and evaluation of disproportionation-induced Pu(VI) self-reduction*

Modeling of disproportionation-induced reduction of 9.7 mM ^{239}Pu(VI) at pH 1.5 [8] is described in the earlier report [2]. The predicted [Pu(VI)]–time curve agrees

Table 4
Dependence of k_V on $[H^+]$ in perchlorate solution[a,b]

pH range	Expression for $[H^+]$ dependence of k_V	a_V (Units)
<(3.8 ± 0.3)	$a_V[H^+]$	4×10^{-3} ($\mathrm{l^2\,mol^{-2}\,s^{-1}}$)
(3.8 ± 0.3)–10	$a_V[H^+]^{-2}$	4×10^{-15} ($\mathrm{mol\,l^{-1}\ s^{-1}}$)
10–(12.8 ± 0.2)	a_V	4×10^{5} ($\mathrm{l\,mol^{-1}\,s^{-1}}$)[b]
>(12.8 ± 0.2)	$a_V[H^+]^4$	1×10^{56} ($\mathrm{l^5\ mol^{-5}\ s^{-1}}$)

[a] Equations are derived using published $\ln k_V$–$\ln[H^+]$ data [2].

[b] Solutions are free of complexing ligands.

with experimental data. Comparison of observed and predicted kinetic parameters (Table 2) shows that disproportionation-induced self-reduction accurately accounts for behavior. Similar agreement is also achieved with a model based on first-order dependence of the self-reduction rate on [Pu(VI)] [1]. However, a first-order dependence is possible only if the concentration of reducing agent is large and essentially constant. In this case, a period of years is required to reach a radiolytic [H_2O_2] that satisfies this requirement.

[Pu(VI)]–time data predicted for disproprotionation-induced self-reduction of 0.1 mM ^{242}Pu(VI) at pH 6 [9] agree with experimental values. The k_{VI} derived from data for k_V (Table 4) is 4.0×10^{-3} $\mathrm{l\,mol^{-1}\,s^{-1}}$; the value after data-fitting is 1.4×10^{-3} $\mathrm{l\,mol^{-1}\,s^{-1}}$. Respective Pu(VI) concentrations observed at 0, 6.3, 10.4, and 110 days are 100, 92, 85, and 42 μM. The corresponding predictions are 100, 91, 86, and 41 μM. Self-reduction at these conditions is accurately described by disproportionation of Pu(VI).

Evaluation of self-reduction for 1.1 mM ^{238}Pu(VI) at pH 0 [11] shows that experimental [Pu(VI)]–time data are not duplicated using the second-order rate law. The k_{VI} derived from data for k_V (Table 4) is of 4.0×10^{-3} $\mathrm{l\,mol^{-1}\,s^{-1}}$. As shown in Table 3, agreement of the predicted [Pu(VI)] with observation is achieved at day 2.73 using a k_{VI} of 2.9×10^{-3} $\mathrm{l\,mol^{-1}\,s^{-1}}$. However, the disproportionation model does not account for continued rapid reduction or for attainment of the [Pu(VI)] observed at day 6.9. This failure and success of the radiolytic model (Section 3.1.2) support the conclusion that self-reduction of ^{238}Pu(VI) is radiolysis-induced at the conditions of the study [11].

3.3. Chemistry and prediction of Pu(VI) self-reduction kinetics

Understanding of Pu(VI) self-reduction is essential for accurate interpretation and modeling of plutonium solution chemistry. Self-reduction of Pu(VI) by both radiolysis and disproportionation adds electrons to the plutonium system and drives the well-known decrease in average oxidation number of plutonium-containing solutions over time. However, significant differences in the extent of reduction are observed in studies at similar conditions. Whereas Pu(III) is formed in one case [10], Pu(V) and Pu(VI) are the only products observed in another [8].

Appearance of different oxidation states in solutions of Pu(V) and Pu(VI) is consistent with the kinetic effect of initial Pu concentration on the rates of two well-known instability pathways of Pu(V) [5]: (1) formation of Pu(IV) and Pu(VI) by disproportionation of Pu(V) and (2) formation of Pu(III) plus Pu(VI) by reaction of Pu(V) and Pu(IV). Behavior of Pu(VI) and Pu(V) solutions converge because Pu(V) is produced during self-reduction of Pu(VI) and Pu(VI) is formed by disproportionation of Pu(V). The initial concentration of Pu(V) or Pu(VI) determines whether or not the [Pu(IV)] formed by disproportionation of Pu(V) satisfies the K_{sp} for precipitation of hydrous oxide at system pH. If $[\mathrm{Pu(VI)}]_0$ is high, the resulting [Pu(V)] is also high and Pu(IV) accumulates until its concentration equals the equilibrium value of hydrous oxide. Continuing precipitation of hydrous oxide maintains a low [Pu(IV)] relative to the [Pu(V)]. Formation of Pu(IV) and Pu(VI) is inherently favored because the rate of the Pu(IV)–Pu(V) reaction is negligible at high [Pu(V)] and low [Pu(IV)]. However, if the initial Pu concentration is insufficient for precipitation of hydrous oxide, product Pu(IV) accumulates and the Pu(IV)–Pu(V) reaction forms Pu(III) and Pu(VI) as reactant concentrations become comparable. Reactions of Pu(V) via both pathways result in reformation of Pu(VI) and lead a progressive decrease in the average oxidation number as electrons are supplied by continuing Pu(VI) self-reduction.

The most rapid self-reduction pathway is followed. Disproportionation is favored at zero time because [Pu(VI)] is at the maximum value and $[H_2O_2]_0$ is inherently small. Disproportionation-induced reduction is replaced by radiolysis-induced reduction if that path becomes more rapid due to the combined effect of increase in radiolytic [H_2O_2] and decrease in [Pu(VI)] over time.

The pathways for disproportionation-induced and radiolysis-induced reduction are characterized by distinctive [Pu(VI)]–time curves. The [Pu(VI)]–time curve for disproportionation-induced reduction at fixed pH is parabolic. The curve for radiolysis-induced reduction is linear if the reaction rate of radiolytic peroxide exceeds the formation rate and sigmoidal if peroxide is formed at a faster rate than it reacts. In all cases, the anticipated [Pu(VI)]–time dependence terminates if the rate is exceeded by that of a competing reaction.

A simple method for predicting the time dependence of Pu(VI) self-reduction is implied by the preceding discussion. Predicted rates of disproportionation- and radiolysis-induced self-reduction are compared; the reaction is expected to follow the more rapid reduction path. Effects of all radiolytic species are included by basing the radiolysis rate on $G_{\mathrm{Pu(VI)}} = 1.18$.

3.4. Pu(VI) reduction in the presence of ^{210}Po

3.4.1. Summary and interpretation of measurements

As part of an extensive investigation of radiolysis effects on plutonium redox chemistry, Pagès measured the time dependence of [Pu(VI)] for 5.26 mM Pu(VI) solutions at pH 0.7 [10]. An alpha dose rate of 3.7×10^{17} $\mathrm{eV\,cm^{-3}\,h^{-1}}$ was achieved by addition of ^{210}Po to the solution. The [Pu(VI)]–time data in Fig. 1 include values obtained both in the presence and absence of

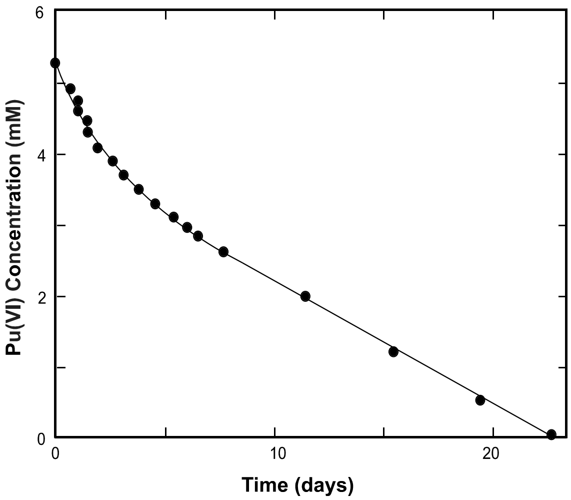

Fig. 1. Comparison of the predicted [Pu(VI)]–time curves (solid line) with measured data for self-reduction of Pu(VI) in a solution containing ^{210}Po [10].

air. Ordinate units are transformed from ions cm^{-3} to M and abscissa units are transformed from eV cm^{-3} to time. Disappearance of Pu(VI) was accompanied by a sequence of maxima in the concentrations of lower-oxidation-state Pu: [Pu(V)] reached a maximum at 3–4 days, [Pu(IV)] reached a maximum at 11–12 days, and [Pu(III)] reached a maximum as concentrations of higher oxidation states fell below detectable limits near day 23.

Results are interpreted using three *G* values for radiolytic reduction of Pu(VI) as defined by instantaneous slopes of the concentration–dose curve [10]. An initial *G* value of 3.20 for weak alpha doses is attributed to formation of Pu(V), a *G* value of 1.60 for intermediate doses ($>2\times10^{19}$ eV cm^{-3}) is assigned to formation of Pu(IV), and a *G* value of 1.10 for high doses ($>7\times10^{19}$ eV cm^{-3}) is associated with formation of Pu(III). The derived *G* values are attributed to different molecular-yield combinations for radiolytic products of water, but the concept was not verified due to unavailability of quantitative data.

3.4.2. Modeling and assessment of Pu(VI) reduction

The proposed interpretation of results in Fig. 1 is counterintuitive and inconsistent with subsequently determined *G* values in Table 1. As noted in the introduction, observation of the maximum radiolysis-induced reduction near zero time is unlikely because the high concentrations of radiolytic reductants necessary for rapid reaction are not present. The reported initial *G* value of 3.20 [10] is significantly greater than the maximum theoretical $G_{\mathrm{Pu(VI)}}$ of 2.22. The shape of the [Pu(VI)]–time data in Fig. 1 is neither linear nor sigmoidal. The results afford an ideal opportunity for testing the predictive method outlined in Section 3.3.

Radiolysis-induced reduction of Pu(VI) by ^{210}Po [10] parallels that for self-reduction by Pu isotopes. The rate of H_2O_2 formation derived from the reported alpha dose rate is 1.5×10^{-4} mol l^{-1} d^{-1}. Modeling predicts that H_2O_2 accumulates in solution and $-R_r$ increases during an initial 2.5 hour period. Thereafter, $-R_r$ is limited by the rate of H_2O_2 formation and [Pu(VI)] decreases at the radiolysis-controlled maximum rate. Calculation using $G_{\mathrm{Pu(VI)}} = 1.18$ yields a constant maximum $-R_r$ of 1.74×10^{-4} mol l^{-1} d^{-1}.

Disproprotionation-induced self-reduction of 5.26 mM Pu(VI) at pH 0.7 [10] is modeled using the second-order rate law. [Pu(VI)]–time results and $-R_d$ values are derived using $k_{\mathrm{VI}} = k_{\mathrm{V}}/4 = 2.5\times10^{-4}$ l mol^{-1} s^{-1}. The initial $-R_d$ is 6.64×10^{-4} mol l^{-1} d^{-1}. Predicted behavior is indicated by representative results. Derived [Pu(VI)] values at 0, 2, 4, and 6, days are 5.26, 4.22, 3.52, and 3.02 mM, respectively. [Pu(VI)] and $-R_d$ are 2.64 mM and 1.74×10^{-4} mol l^{-1} d^{-1} at day 8 and progressively decrease with time.

The disproportionation-induced rate exceeds the maximum radiolysis-induced rate prior to day 8 and is the predicted path for Pu(VI) self-reduction during that period. Beyond that point, the constant radiolysis-induced reduction is more rapid and dominant. $[\mathrm{Pu(VI)}]_0$ is slightly less than the measured solubility (~6 mM) of hydrous oxide at pH 0.7 [18]. Therefore, continuing self-reduction of recycled Pu(VI) is expected to result in formation of Pu(III) and to drive the [Pu(VI)] below detectable limits near day 23. Maxima in the concentrations of Pu(V), Pu(IV), and Pu(III) are inherent consequences of Pu(VI) self-reduction and the sequence of reactions outlined in Section 3.3. Agreement of predicted [Pu(VI)]–time behavior with experimental data in Fig. 1 is excellent. The solid line is predicted by modeling; it is not derived by fitting the experimental data.

Accurate prediction of the [Pu(VI)]–time curve using initial conditions and independent parameters demonstrates that the proposed method for modeling Pu(VI) self-reduction is valid and applicable to real systems. The resulting interpretation of data for Pu(VI) solutions containing ^{210}Po differs substantially from that proposed in the original report [10].

3.5. Competition of reaction pathways

Two competing pathways exist for self-reduction of Pu(VI). Radiolysis-induced reduction is favored by the presence of short-lived Pu isotopes. Pu(VI) disproportionation is generally favored by high concentrations of long-lived isotopes, but modeling is necessary for accurate prediction of behavior.

In an effort to identify conditions that favor the respective pathway, rates of the two reduction reactions have been calculated within a limited matrix bounded by $[\mathrm{Pu(VI)}]_0$ values of 0.1–100 mM and pH values of 0 to 6.

Predictions are based on the assumption that the Pu(VI)–H_2O_2 rate law is applicable over this pH range. An isotopic mixture found in typical weapons-grade Pu [19] is adopted as the Pu source. The specific alpha activity is 2.8 GBq g^{-1} and $+R_{H_2O_2} = 4.9 \times 10^{-3}$ $mol\,l^{-1}\,d^{-1}$ [Pu]. A complex dependence of k_{VI} on $[H^+]$ is anticipated because k_V and k_{VI} reach minima at pH 3.5–4.0 with values that are 10^4 less than those at pH 0 and 6 [2].

Modeling shows that $-R_{H_2O_2}$ consistently exceeds $+R_{H_2O_2}$ for weapon-grade Pu. Therefore, radiolysis-induced reaction proceeds at the maximum rate determined by the kinetics of peroxide formation. Although disproportionation predominates for 0.1 M Pu(VI) solutions, calculations indicate that radiolysis-induced reaction is more rapid and favored in a narrow pH zone between pH 3.5 and 4.0. The predicted size of this zone progressively increases with decreasing $[Pu(VI)]_0$ and extends from below pH 2 to beyond pH 5 for 0.1 mM $[Pu(VI)]_0$. However, radiolysis reduced rates may be significantly lower than predicted because of alpha-energy losses. Molecular yield is sensitive to container geometry and to self-absorption by solids. Such energy losses may contribute to lower-than-expected radiolytic reduction rate for ^{238}Pu(VI).

3.6. Conclusions

Attention is drawn to the importance of understanding and accurately describing the chemistry and kinetics of Pu(VI) self-reduction and the electron source that drives the well-known decrease in average oxidation number of plutonium solutions over time. Modeling results show that the generally accepted description of Pu(VI) self-reduction is substantially inaccurate. Two distinctly different reduction pathways lead to the same net redox reaction for Pu(VI) (Eq. (2)). Alternative pathways are characterized by shapes of the [Pu(VI)]–time curves and follow sequentially in some cases. Results suggest that disproportionation-induced reaction is the predominant pathway for self-reduction of long-lived Pu(VI) isotopes in acidic and near-neutral solutions.

The utility of kinetic modeling for interpreting and quantifying the chemistry and kinetic of plutonium solutions is demonstrated by accurate prediction of the [Pu(VI)]–time dependence for self-reduction of several Pu(VI) isotopes. This success confirms two important features of disproportionation-induced reduction: that $-d[Pu(VI)]/dt$ is proportional to $[Pu(VI)]^2$ and that the proportionality constant is remarkably similar to k_V for disproportionation of Pu(V) [2,3].

Fundamental tenets of plutonium chemistry are challenged by this study. Results show that alpha-induced reaction is neither the only pathway nor the predominant pathway for Pu(VI) self-reduction. Questions arise about the adequacy of using equilibrium concepts to describe the redox chemistry of Pu in aqueous solution. An extensive reassessment of data for plutonium solutions seems merited.

References

[1] T.W. Newton, D.E. Hobart, J. Nucl. Mater. 334 (2004) 222.
[2] J.M. Haschke, J. Nucl. Mater. 334 (2004) 225.
[3] J.M. Haschke, V.M. Oversby, J. Nucl. Mater. 305 (2002) 187.
[4] C. Keller, H. Seifert, Angew. Chem. 8 (1969) 279.
[5] J.M. Cleveland, The Chemistry of Plutonium, American Nuclear Society, La Grange Park, IL, 1979 (Chapter 3).
[6] R. Knopp, V. Neck, J.I. Kim, Radiochim. Acta. 86 (1999) 101.
[7] H. Christensen, Nucl. Technol. 124 (1998) 165.
[8] T.W. Newton, D.E. Hobart, P.D. Palmer, Radiochim. Acta 39 (1986) 139.
[9] D.T. Reed, D.G. Wygmans, S.B. Aase, J.E. Banazak, Radiochim. Acta 82 (1998) 109.
[10] M. Pagès, J. Chim. Phys. 59 (1962) 63.
[11] K. Büpplemann, J.I. Kim, C. Lierse, Radiochim. Acta 44&45 (1988) 65.
[12] R.J. Lemire, J. Fuger, H. Nitsche, P. Potter, M.H. Rand, J. Rydberg, K. Spahiu, J.C. Sullivan, W.J. Ullman, P. Vitorge, H. Wanner, Chemical Thermodynamics of Neptunium and Plutonium, Elsevier, Amsterdam, 2001, p. 55.
[13] R.C. Weast, CRC Handbook of Chemistry and Physics, CRC Press, Boca Raton, FL, 1988, p. D69.
[14] J.M. Haschke, R.L. Bassett, Radiochim. Acta 90 (2002) 505.
[15] H. Nitsche, K. Roberts, R. Xi, T. Prussin, K. Beacraft, I.A. Mahamid, H.B. Silbers, S.A. Carpenter, R.C. Gatti, C.F. Novak, Radiochim. Acta 66&67 (1994) 3.
[16] R.J. McMahon, Science 299 (2003) 833.
[17] T.K. Keenan, J. Phys. Chem. 61 (1957) 1117.
[18] D. Rai, Radiochim. Acta 35 (1984) 97.
[19] Safety Report Series No. 9, Safe Handling and Storage of Plutonium, International Atomic Energy Agency, Vienna (1998) p. 13.